Photoacoustic effect in a stratified atmosphere

Wenyu Bai and Gerald J. Diebold

Phys. Rev. E **98**, 032125 — Published 20 September 2018

DOI: 10.1103/PhysRevE.98.032125

Photoacoustic effect in a stratified atmosphere

Wenyu Bai* and Gerald J. Diebold
*Department of Chemistry, Brown University, 324 Brook Street, Providence, Rhode Island 02912, USA**

The photoacoustic effect is usually studied in an isotropic medium on a laboratory scale. However, it is possible to use optical sources to launch pressure perturbations in the atmosphere consisting of both acoustic and gravity waves. Here, photoacoustic theory is extended to incorporate the effects of a stratified atmosphere and a gravitational field on launching and propagation of pressure waves in the atmosphere. Properties of pressure waves corresponding to several optical excitation schemes are investigated. The acoustic component of the optically launched pressure waves is explored separately to delineate its properties from those found without the effects of a gravitational field.

Keywords: photoacoustics, atmosphere, anisotropic medium, Green's function

I. INTRODUCTION

The photoacoustic effect refers to the generation of sound by absorption of optical radiation, which was first reported by Alexander Graham Bell in 1880 in his invention of the photophone [1]. However, it was not until 1970's, after the invention of the laser, that the photoacoustic effect received considerable research interest in the fields of spectroscopy and trace gas detection [2–4]. The last decade has witnessed additional interest in the photoacoustic effect owing mainly to its unique advantages in noninvasive biomedical imaging [5, 6].

Apart from laboratory applications, the photoacoustic effect has been shown to be manifest in natural phenomena. For example, the mysterious "hissing" sound occurring concurrently with the flash of meteors has been ascribed to a photoacoustic mechanism [7, 8]. Notably, the source term of the photoacoustic wave equation indicates that a moving source with constant intensity can also broadcast acoustic waves [9, 10]. Such moving sources are associated with the widely-observed pressure disturbance induced by the motion of moon shadow during a solar eclipse [11] and the rotation of the earth terminator [12]. Other events such as the volcanic eruption [13] and nuclear detonation [14] also bear a striking resemblance to the pulsed-mode photoacoustic excitation.

The photoacoustic theory in a fluid is described by an inhomogeneous wave equation for pressure with a source term proportional to the time derivative of the rate of heat deposition per unit volume [15–17]. However, the photoacoustic theory formulated in isotropic media cannot be directly applied to atmospheric pressure waves since the atmosphere is stratified and the length scale of the pressure waves is often comparable to or larger than the characteristic length of the stratification [18]. As well, the presence of the gravitational field complicates the propagation of the pressure disturbance. Apart from acoustic waves, there also exist low frequency gravity waves supported by the buoyant force [19]. The so-called acoustic-gravity wave has been explored before by geologists and is of primary interest in its effects on atmospheric circulation and local surface turbulence [14, 20]. However, the wave's behavior unique to optical excitation and its connection with the photoacoustic effect have not been systematically studied to our best knowledge. Furthermore, photoacoustic remote sensing of the marine environment and the possible photoacoustic air-to-submarine communication can be expected to require an airborne laser which as it traverses the atmosphere can introduce pressure perturbations [21]. The interpretation of such pressure waves requires the incorporation of atmospheric stratification into the equations of linear acoustics.

The aim of this paper is to extend the photoacoustic theory to the stratified atmosphere, investigate how the medium anisotropy will affect the generation of pressure disturbances, and examine the atmosphere's response to several typical methods of optical excitation. In particular, the acoustic component of the pressure disturbances is studied as a direct comparison with the ordinary photoacoustic effect. Section II uses the equations of linear acoustics to give the governing equation for pressure disturbances induced by optical excitation in the atmosphere. A Green's function is derived and the effect of a boundary is discussed. Section III gives examples of optically launched atmospheric waves including the cases for pulsed and low frequency monopole radiator. In Section IV, the high frequency approximation to the governing equation is derived and applied to the cases of a vertically directed light beam and a monopole source. Section V gives a summary of the results.

II. GOVERNING EQUATION AND GREEN'S FUNCTION

A. Derivation of the governing equation

Consider a flat earth, taken to be a hard surface, and an isothermal, windless atmosphere as illustrated in Fig. 1. The influence of earth rotation is neglected here since the Rossby waves generated by the Coriolis forces are characterized by extremely low frequencies and long wavelengths. The excitation of such waves with signifi-

* Email: wenyu_bai@brown.edu

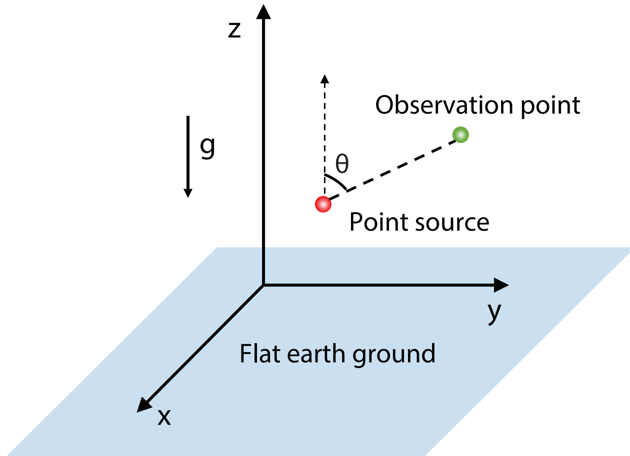

FIG. 1. (Color online) Geometry of the theoretical model with the gravitational force antiparallel to the z axis and the earth taken to be a flat, perfect reflector.

cant amplitudes is thus not expected. [22]. Suppose the optically excited pressure disturbance is small enough so that the linearized conservation equations are given by

$$\rho_0 \frac{\partial \mathbf{u}_1}{\partial t} = -\nabla p_1 - \rho_1 \mathbf{g},$$
$$\frac{\partial p_1}{\partial t} + u_{1z}\frac{\partial p_0}{\partial z} = c^2\left(\frac{\partial \rho_1}{\partial t} + u_{1z}\frac{\partial \rho_0}{\partial z}\right) + \frac{\beta c^2}{C_P}H,$$
$$\frac{\partial \rho_1}{\partial t} = -u_{1z}\frac{\partial \rho_0}{\partial z} - \rho_0 \nabla \mathbf{u}_1, \tag{1}$$

where subscript 0 indicates a hydrostatic variable and the subscript 1 refers to small disturbance, ρ is the density, $\mathbf{u} = (u_x, u_y, u_z)$ is the particle velocity, p is the pressure, $\mathbf{g} = (0, 0, g)$ is the gravitational field, β is the isothermal expansion coefficient, C_P is the specific heat capacity at constant pressure, and H, the heating function, is the optical power absorbed per unit volume. The first of Eqs. 1 is a vector differential equation that describes the conservation of momentum along the x, y, z directions. The second and third equations are the conservation equations for energy and mass, respectively.

The distributions of hydrostatic pressure p_0 and density ρ_0 obey the following relations,

$$\frac{\partial p_0}{\partial z} = -g\rho_0, \tag{2a}$$
$$\frac{\partial \rho_0}{\partial z} = -\frac{\gamma g}{c^2}\rho_0, \tag{2b}$$

where γ is the ratio of specific heat capacities at constant pressure and volume. Note that p_0 and ρ_0 are related via the adiabatic sound speed $c = \sqrt{\gamma p_0/\rho_0}$, which, together with Eqs. 2a and 2b, gives

$$p_0 = P_s e^{-z/h} \qquad \text{and} \qquad \rho_0 = \varrho_s e^{-z/h}, \tag{3}$$

where h is a characteristic height defined as $h = c^2/(\gamma g)$, which in the earth atmosphere is roughly 8 km. Here P_s and ϱ_s are the hydrostatic pressure and density at the sea level.

Equations 3 can be used to eliminate the variables p_0 and ρ_0 from Eqs. 1, leaving five unknowns u_{1x}, u_{1y}, u_{1z}, p_1, and ρ_1, which can then be decoupled by manipulation of the five conservation equations. A partial differential equation for the pressure perturbation p_1 is accordingly obtained as

$$\left[\frac{\partial^4}{\partial t^4} - c^2\frac{\partial^2}{\partial t^2}\nabla^2 - \frac{\gamma g \partial^3}{\partial t^2 \partial z} - (\gamma-1)g^2\left(\frac{\partial^2}{\partial x^2} + \frac{\partial^2}{\partial y^2}\right)\right]p_1$$
$$= \frac{\beta c^2}{C_P}\left(\frac{\partial^3 H}{\partial t^3} - g\frac{\partial^2 H}{\partial t \partial z}\right). \tag{4}$$

Compared with the source term of the ordinary photoacoustic wave equation for non-stratified fluids [15], Eq. 4 includes an additional source term dependent on both the gravitational acceleration and the vertical dependence of the heating function. It is easy to verify that Eq. 4 reduces to the well-known photoacoustic wave equation for fluids [15] as g vanishes.

If a new variable Π is defined as $\Pi = \exp[z/(2h)]\, p_1$, Eq. 4 can be reduced to

$$\left[\frac{1}{c^2}\frac{\partial^4}{\partial t^4} - \frac{\partial^2}{\partial t^2}\nabla^2 + \frac{\omega_2^2}{c^2}\frac{\partial^2}{\partial t^2} - \omega_1^2\left(\frac{\partial^2}{\partial x^2} + \frac{\partial^2}{\partial y^2}\right)\right]\Pi$$
$$= \frac{\beta e^{z/(2h)}}{C_P}\left(\frac{\partial^3 H}{\partial t^3} - g\frac{\partial^2 H}{\partial t \partial z}\right), \tag{5}$$

where $\omega_1 = \sqrt{(\gamma-1)g/(\gamma h)}$ is the so-called Brunt-Väisälä frequency [23] and $\omega_2 = 1/2\sqrt{\gamma g/h}$. Their values in an isothermal atmosphere are roughly 0.018 rad / s and 0.02 rad / s corresponding to oscillations with periods around 5.8 min and 5.2 min, respectively. It is noted that the substitution of p_1 with Π has some physical significance. Since the potential energy associated with the fluid compression is proportional to Π^2 with the prefactor $1/(2c^2\varrho_s)$ being a constant, Π is thus required to be a squared integrable function and is a physically more preferable variable to work with than p_1.

Fourier transformation of Eq. 5 with the convention $\tilde{f}_\omega = 1/\sqrt{2\pi}\int f(t)\exp(i\omega t)dt$ results in

$$\left(\frac{\partial^2}{\partial x^2} + \frac{\partial^2}{\partial y^2} + \frac{\omega^2}{\omega^2 - \omega_1^2}\frac{\partial^2}{\partial z^2} + \frac{\omega^2 - \omega_2^2}{\omega^2 - \omega_1^2}\frac{\omega^2}{c^2}\right)\tilde{\Pi}$$
$$= \frac{i\beta\omega e^{z/(2h)}}{C_P(\omega^2 - \omega_1^2)}\left(\omega^2\tilde{H} + g\frac{\partial \tilde{H}}{\partial z}\right), \tag{6}$$

where $\tilde{\Pi}$ and $\tilde{H}$ are the Fourier transform of Π and H. Equation 6 can be used to determine the frequency domain solutions for various forms of the heating function. The result can then be Fourier transformed to give time domain solutions to Eq. 5.

B. Free space Green's function

In this section, the Green's function for Eq. 6 is derived for free space without the presence of a reflecting surface.

The frequency domain Green's function $\tilde{G}_\omega(\mathbf{r};\mathbf{r}_0)$ for Eq. 5 satisfies the following equation

$$\left(\frac{\partial^2}{\partial x^2}+\frac{\partial^2}{\partial y^2}+\frac{\omega^2}{\omega^2-\omega_1^2}\frac{\partial^2}{\partial z^2}+\frac{\omega^2-\omega_2^2}{\omega^2-\omega_1^2}\frac{\omega^2}{c^2}\right)\tilde{G}_\omega(\mathbf{r};\mathbf{r}_0) = \delta(\mathbf{r}-\mathbf{r}_0), \tag{7}$$

where $\mathbf{r}$ and $\mathbf{r}_0$ refer to the positions of the observation point and the source point, respectively. By taking the Fourier transform of the z variable with the convention $\tilde{f}_{k_z} = 1/\sqrt{2\pi}\int f(z)\exp(ik_z z)dz$, we have

$$\left(\frac{\partial^2}{\partial x^2}+\frac{\partial^2}{\partial y^2}+F^2\right)\tilde{G}_{\omega,k_z}(x,y;x_0,y_0) = \frac{1}{\sqrt{2\pi}}e^{ik_z z_0}\delta(x-x_0)\delta(y-y_0), \tag{8}$$

where

$$F = \sqrt{\hat{\alpha}\left(\frac{\hat{\beta}}{\hat{\alpha}}\frac{\omega^2}{c^2}-k_z^2\right)},$$
$$\hat{\alpha} = \frac{\omega^2}{\omega^2-\omega_1^2},$$
$$\hat{\beta} = \frac{\omega^2-\omega_2^2}{\omega^2-\omega_1^2}.$$

Note that Eq. 8 is a two-dimensional Helmholtz equation whose solution can be found as [24]

$$\tilde{G}_{\omega,k_z}(x,y;x_0,y_0) = -\frac{i}{4\sqrt{2\pi}}e^{ik_z z_0}H_0^{(1)}(Fd), \tag{9}$$

where $d = \sqrt{(x-x_0)^2+(y-y_0)^2}$, and $H_0^1(z)$ is the Hankel function of the first kind. Under the convention of the Fourier transform used in this paper, Eq. 9 describes an outwardly expanding wave.

Inverse Fourier transformation of Eq. 9 with respect to k_z gives

$$\tilde{G}_\omega(\mathbf{r};\mathbf{r}_0) = -\frac{i}{4\pi}\int_0^\infty H_0^{(1)}\left[\sqrt{\hat{\alpha}\left(\frac{\hat{\beta}}{\hat{\alpha}}\frac{\omega^2}{c^2}-k_z^2\right)}d\right]\times \cos\left[k_z(z-z_0)\right]dk_z, \tag{10}$$

where the parity symmetry of the F term with respect to k_z is used to write $\tilde{G}_\omega$ as a Fourier cosine transform. The integral in Eq. 10 can be found in standard integral tables [25], yielding

$$\tilde{G}_\omega(\mathbf{r};\mathbf{r}_0) = -\frac{1}{4\pi}\sqrt{\frac{1}{\hat{\alpha}}}\frac{1}{R}e^{i\omega\sqrt{\hat{\beta}}R/c}, \tag{11}$$

where $R(\mathbf{r};\mathbf{r}_0) = \sqrt{(x-x_0)^2+(y-y_0)^2+(z-z_0)^2/\hat{\alpha}}$. The appearance of $1/\hat{\alpha}$ within R suggests an anisotropic behavior along the z direction which is discussed later. It is noted that when $\omega \gg \omega_2$ both $\hat{\alpha}$ and $\hat{\beta}$ approach the unity, making $\tilde{G}_\omega$ converge to the Green's function for a three-dimensional wave equation.

One interesting finding is that when the observation point is directly above or below the impulsive source point, Eq. 11 becomes

$$\tilde{G}_\omega(z;z_0) = -\frac{1}{4\pi}\frac{1}{|z-z_0|}e^{i\sqrt{(\omega/c)^2-(\omega_2/c)^2}|z-z_0|}, \tag{12}$$

which is similar to the Green's function for the frequency domain Klein-Gordon equation, a relativistic version of the Schrödinger equation whose solution has been widely studied. Inverse Fourier transformation of Eq. 12, according to Ref. [24], yields

$$\bar{G}(z,t;z_0,t_0) = -\frac{1}{4\pi}\Bigg\{\frac{\delta(\tau-|z-z_0|/c)}{|z-z_0|}-\frac{\omega_2 J_1\left[\omega_2\sqrt{\tau^2-(|z-z_0|/c)^2}\right]}{c\sqrt{\tau^2-(|z-z_0|/c)^2}}\times u(\tau-|z-z_0|/c)\Bigg\}, \tag{13}$$

where $\tau = t-t_0$, t_0 is the time of initiation of the instantaneous point source, J_1 is the first order Bessel function of the first kind and u is the Heaviside function. The above equation describes a delta pulse followed by a wake which is a characteristic feature for the acoustic-gravity wave.

Of particular note is that Eq. 13 cannot be simply regarded as the atmosphere's response to an impulsive source since the source term in Eq. 5 is not proportional to the heating function but involves its temporal and spatial derivatives. This fact can be exemplified by the phenomenon that the photoacoustic response to an impulsive source in a three-dimensional geometry is a bipolar acoustic wave – a compression followed by rarefaction, while the first term in Eq. 13 is merely a unipolar wave. Furthermore, when calculating the Green's function for the time domain Eq. 5, the Green's function in the frequency domain should be divided by another factor $\omega^2-\omega_1^2$ before conducting the inverse Fourier transformation, that is,

$$G(\mathbf{r},t;\mathbf{r}_0,t_0) = \frac{1}{2\pi}\int_{-\infty}^{\infty}\frac{\tilde{G}_\omega(\mathbf{r};\mathbf{r}_0)}{\omega^2-\omega_1^2}e^{-i\omega\tau}d\omega = \frac{1}{\pi}\mathrm{Re}\left[\int_0^\infty\frac{\tilde{G}_\omega(\mathbf{r};\mathbf{r}_0)}{\omega^2-\omega_1^2}e^{-i\omega\tau}d\omega\right], \tag{14}$$

where the second equation is derived based on the fact that $\tilde{G}_\omega(\mathbf{r};\mathbf{r}_0)$ is a Hermitian function with respect to ω, that is, it satisfies $\tilde{G}_\omega(\mathbf{r};\mathbf{r}_0) = \tilde{G}^*_{-\omega}(\mathbf{r};\mathbf{r}_0)$. The solution to Eq. 4 can be obtained by convoluting Eq. 14 with the source term in Eq. 5 with the result multiplied by $\exp\left[-z/(2h)\right]$.

It is difficult to obtain a closed-form expression for the integral in Eq. 14, but it is possible to determine some

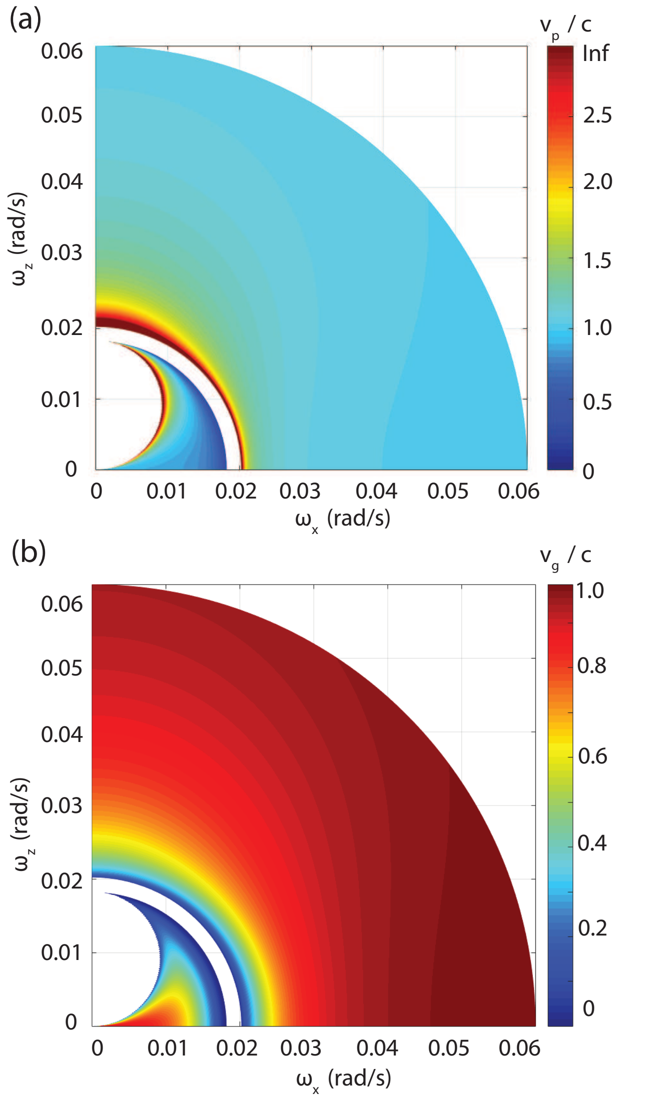

FIG. 2. (Color online) Phase (upper plot) and group (lower plot) velocities as a function of $\omega_x = \omega \sin\theta$ and $\omega_z = \omega\cos\theta$. The phase velocity varies from zero to the infinity while its color plot is truncated at $v_p/c = 3$ to make clear the details of the distribution. Within the blank areas at the left bottom corners, the velocities become imaginary indicating evanescent wave behavior.

properties of $G(\mathbf{r}, t; \mathbf{r}_0, t_0)$ by investigating the behavior of the integrand in the complex ω plane. First note that there exist six singularities for the integrand which are at $\pm\omega_1, \pm\omega_2$ and $\pm\omega_1\cos\theta$ where θ is the polar angle of the vector $\mathbf{r}-\mathbf{r}_0$ as depicted in Fig. 1. Importantly, no poles appear in the upper complex plane, making Eq. 14 satisfy the causality principle since it is then possible to close the integration contour in the upper plane when $t < t_0$, resulting in a value of zero for the integral [24]. Second, in certain frequency bands $(0, \omega_1 |\cos\theta|)$ and (ω_1, ω_2), the integrand behaves as an exponentially decaying function instead of being progressive. The second frequency band results from the fact that for a pure gravity wave, or a wave with the oscillation frequency so low that the rate of change of ρ_1 barely affects the continuity equation, the maximum frequency that the atmosphere can support is the Brunt-Väisälä frequency ω_1 [19]. The first frequency band gives a hint of the radiation pattern for a low-frequency point source. Suppose a point source located at the origin oscillates in amplitude at an angular frequency $\omega_0 (< \omega_1)$. Its radiation will be excluded from a head-to-head cone-shaped region as illustrated in Fig. 4(b) with the cone angle being $\pi - 2\arccos(\omega_0/\omega_1)$, which is in striking contrast to that from a photoacoustic monopole [15]. Third, it is also worthwhile investigating the anisotropic dispersion of the phase and group velocities v_p and v_g along the direction of $\mathbf{r}-\mathbf{r}_0$ [19, 26]. It can be shown from the exponent of Eq. 11 that

$$v_p = \frac{\omega}{k} = \frac{c}{\sqrt{\hat{\beta}\left(1 - \omega_1^2\cos^2\theta/\omega^2\right)}}, \qquad \text{and} \tag{15a}$$

$$v_g = \frac{\partial\omega}{\partial k} = \frac{c\sqrt{\hat{\beta}\left(1 - \omega_1^2\cos^2\theta/\omega^2\right)}\left(\omega^2 - \omega_1^2\right)^2}{\left(\omega^2 - \omega_1^2\right)^2 + \omega_1^2\left(\omega_2^2 - \omega_1^2\right)\sin^2\theta}, \tag{15b}$$

where k is the magnitude of the wave number vector. The anisotropic dispersion of v_p and v_g are plotted in Fig. 2. It is clear that there exist two forbidden bands in which the wave is evanescent. In the regime of $\omega_1 |\cos\theta| < \omega < \omega_1$, the phase velocity decreases monotonically from infinity to zero, and the group velocity exhibits some concave behavior with the maximum magnitude still being subsonic. When $\omega > \omega_2$, both velocities asymptotically approach the sound speed, which is consistent with the fact that when $\omega \gg \omega_2$, Eq. 4 converges to a three-dimensional photoacoustic wave equation.

C. Inclusion of a reflecting surface

Reflection occurs when the pressure disturbance travels to the earth surface where the vertical particle velocity u_z vanishes. From the first of Eqs. 1, together with the relation for the adiabatic sound speed $c^2 = p_1/\rho_1$, the boundary condition for p_1 at $z = 0$ can be formulated as

$$\frac{\partial p_1}{\partial z} + \frac{g}{c^2} p_1 = 0, \tag{16}$$

whose corresponding form in terms of Π is given by

$$\frac{\partial \Pi}{\partial z} + A\Pi = 0, \tag{17}$$

where $A = (1/\gamma - 1/2)/h$.

Of note is that a velocity potential cannot be defined in this case as a result of the existence of the gravitational field which results in a pressure disturbance that is a combination of longitudinal (acoustic) and transverse (gravity) wave: the velocity field is not purely irrotational.

To incorporate the effects of the boundary condition, a generalized approach is to decompose the Green's function into the weighted summation or integral of its eigenfunctions, and then apply the boundary condition to each eigenfunction or their weighting coefficients to make each eigenfunction or their linear combination satisfy the boundary condition. Here, a more straightforward method introduced in Ref. [27] is used. The idea is to define a Robin-to-Dirichlet operator $\hat{T} = \partial/\partial z + (1/\gamma - 1/2)/h$. Since Eq. 6 is a linear equation with all coefficients being constants, the function $g = \hat{T}\tilde{\Pi}$ will satisfy Eq. 6 with $\hat{T}$ acting on the source term together with a Dirichlet boundary condition. If the inverse operator $\hat{T}^{-1}$ and the function g can be found, the solution for $\tilde{\Pi}$ can then be derived as $\tilde{\Pi} = \hat{T}^{-1}g$, a process called the Dirichlet-to-Robin transform.

Following the above procedure, it is found that the Green's function for Eq. 6 with a reflecting earth ground can be written as

$$\tilde{G}_{\omega,R} = \tilde{G}_\omega(z - z_0) + \tilde{G}_\omega(z + z_0) + \hat{T}_z^{-1}\tilde{G}_\omega(z + z_0), \quad (18)$$

where only the z coordinate is written out for simplicity and the last term is

$$T_z^{-1}\tilde{G}_\omega(z + z_0) = \int_0^z e^{-A\varepsilon}\tilde{G}\left[z + (z_0 - \varepsilon)\right] d\varepsilon - e^{-2Az}\int_{-z}^{\infty} e^{-A\varepsilon}\tilde{G}\left[z + (z_0 + \varepsilon)\right] d\varepsilon.$$

The first two terms in Eq. 18 constitute a Green's function for the Neumann boundary condition in which the second term corresponds to a "echo-type" reflected wave from a hard surface. The third term, which results from the presence of a gravitational field, represents a "ringing-type" reflected wave. It corresponds to the interference of waves emanating from a series of "ghost" sources lying along $(-z_0, z - z_0)$ and $(-\infty, z - z_0)$. It is interesting to see that such "ringing" wave will disappear in a medium with $\gamma = 2$. Given Eq. 18, numerical integration can then be carried out to obtain the Green's function and its convolution with specific source terms.

III. RESPONSE TO VARIOUS OPTICAL SOURCES

It is of interest to investigate how the atmosphere will respond to the pulsed or amplitude modulated, continuous optical radiation. In this section, pressure waves resulting from several methods of optical excitation are determined and compared with the laboratory-scale photoacoustic waves. In all calculations, the Green's function for free space is used. Pressure waves generated with the presence of the ground surface can be obtained numerically by means of the Dirichlet-to-Robin transform introduced above.

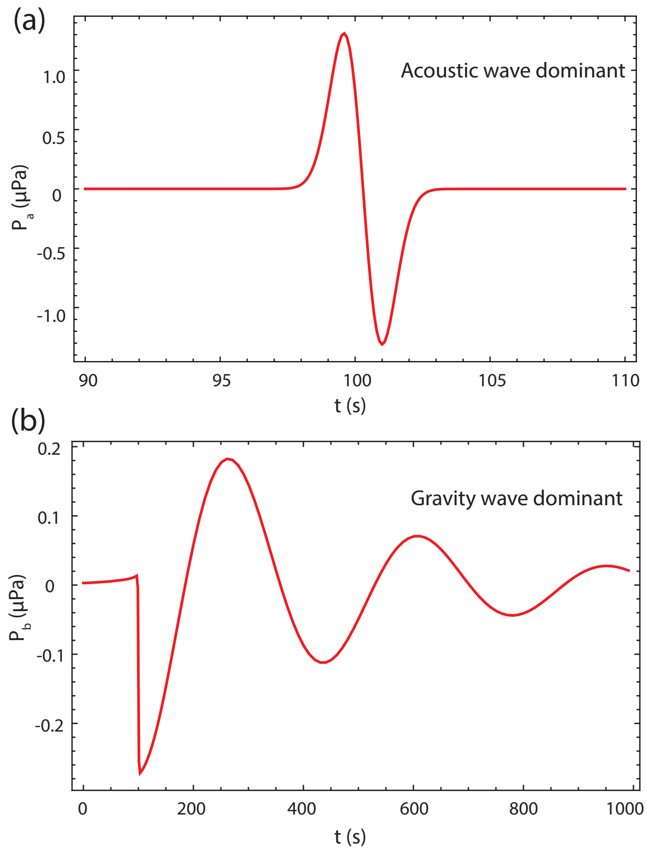

FIG. 3. Pressure versus time for a Gaussian point source associated with the two source terms in Eq. 4. The source is positioned at $(0, 0, 100\ \mathrm{m})$ with $t_s = 100$ s, $\sigma = 1$ s, and $E_0 = 1$ kJ. The observation point is located 100 m below the source. Other physical parameters are taken as $g = 9.8$ m/s^2, $\gamma = 1.4$, $\beta = 0.0034$ K^{-1}, $c = 340$ m/s, $C_p = 1005$ J/kg/K. It is noted that the first source term gives rise to an acoustically dominant wave with the waveform resembling the three-dimensional photoacoustic wave for a pulsed Gaussian point source [10], while the second source term results in a long-tailed, low-frequency wave that is gravity wave dominant.

A. Gaussian point source

For a point source with a Gaussian time profile positioned at $\mathbf{r}_s = (0, 0, z_s)$, the heating function can be written as

$$H(\mathbf{r}, t) = \frac{E_0}{\sqrt{\pi}\sigma}\delta(x)\delta(y)\delta(z - z_s)e^{-(t-t_s)^2/\sigma^2}, \quad (19)$$

where E_0 is the deposited optical energy at the source position, σ is the characteristic duration of the impulsive source, and t_s is the time when the source intensity reaches its maximum. The method of Green's function yields

$$p(\mathbf{r},t) = \frac{\beta e^{-z/(2h)}}{C_P}\int_0^t\int G(\mathbf{r},t;\mathbf{r}_0,t_0)e^{z_0/(2h)}\times \left(\frac{\partial^3}{\partial t_0^3} - g\frac{\partial^2}{\partial t_0 \partial z_0}\right)H(\mathbf{r}_0,t_0)d\mathbf{r}_0 dt_0 = e^{-z/(2h)}\,\mathrm{Re}\left[\hat{p}_a(\mathbf{r},t)+\hat{p}_b(\mathbf{r},t)\right], \quad (20)$$

where

$$\hat{p}_a(\mathbf{r},t) = e^{z_s/(2h)}\Gamma\int_0^\infty\int_0^t \frac{\tilde{G}_\omega(\mathbf{r};\mathbf{r}_0)}{\omega^2-\omega_1^2} \times \frac{\partial^3 e^{-(t_0-t_s)^2/\sigma^2}}{\partial t_0^3}e^{-i\omega(t-t_0)}dt_0 d\omega,$$

$$\hat{p}_b(\mathbf{r},t) = \Gamma\int_0^\infty\int_0^t \frac{g}{\omega^2-\omega_1^2}\frac{\partial}{\partial z_0}\left[\tilde{G}_\omega(\mathbf{r};\mathbf{r}_0)e^{z_0/(2h)}\right]_{z_0=z_s} \times \frac{\partial e^{-(t_0-t_s)^2/\sigma^2}}{\partial t_0}e^{-i\omega(t-t_0)}dt_0 d\omega,$$

where $\Gamma = \beta E_0/(\pi\sqrt{\pi}\sigma C_P)$. The t_0 integration yields a function of ω that is compactly supported along the real axis which enables a rapidly convergent numerical integration for the ensuing ω integral.

Pressure waveforms corresponding to $\hat{p}_a$ and $\hat{p}_b$ are plotted in Fig. 3. It can be seen that the pressure associated with the first source term is dominant by an acoustic wave, which results from the fact that the third order time derivative corresponds to a weighting factor ω^3 in the frequency domain, which amplifies the contribution of high frequency components and weakens the contribution of the low frequency components of the wave. The second source term, on the other hand, is related to the gravity wave which features a long tail and a slowly-varying waveform.

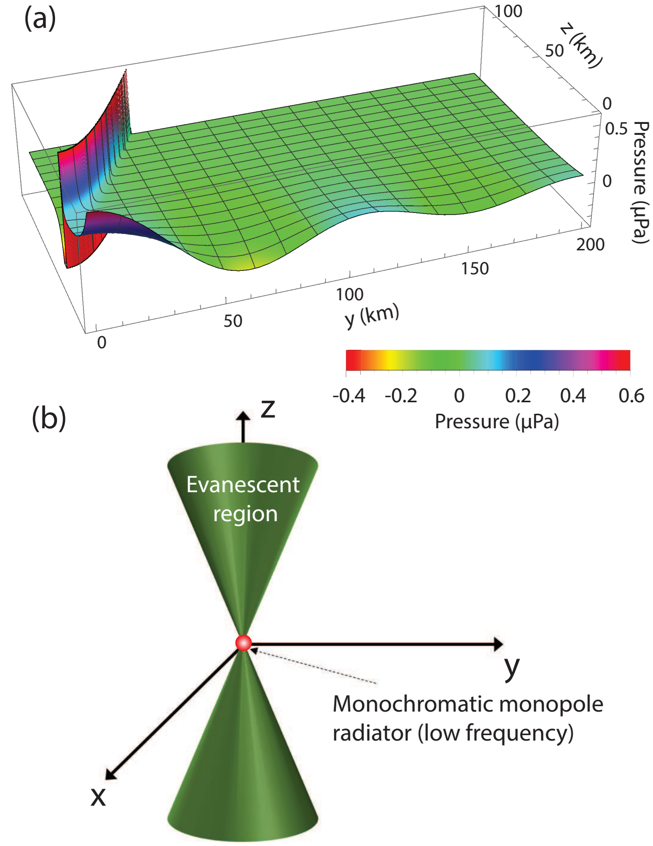

FIG. 4. (Color online) (a) Pressure distribution on the yz plane with $x = 20$ km and (b) the radiation pattern for a low-frequency monochromatic monopole radiator placed at the origin. Plot (a) corresponds to the pressure distribution from a point source with its intensity oscillating at $f_0 = 2.6$ mHz Other parameters are the same as Fig. 3 except that $P_0 = 1$ MW and $t = 100$ s. Plot (b) shows that for point sources with $\omega_0 < \omega_1$ the excited pressure wave will be evanescent within the cones.

B. Low frequency monochromatic monopole radiator

Consider a point source at $\mathbf{r}_s = (0,0,z_s)$ whose intensity varies at an angular frequency ω_0; its heating function can be written as

$$H(\mathbf{r},t) = P_0\left[1+\cos(\omega_0 t)\right]\delta(x)\delta(y)\delta(z-z_s), \quad (21)$$

where P_0 is the absorbed energy per unit time. Since only the time-varying part of the heating function contributes to the pressure, it is preferable to write the heating function as

$$H(\mathbf{r},t) = P_0 e^{-i\omega_0 t}\delta(x)\delta(y)\delta(z-z_s) = e^{-i\omega_0 t}\tilde{H}_s(\mathbf{r}) \quad (22)$$

with the pressure corresponding to the real part of the solution.

Owing to the assumed linearity of the system, the solution to Eq. 5 can be written as $\Pi = \tilde{\Pi}e^{-i\omega_0 t}$ where $\tilde{\Pi}$ satisfies Eq. 6 with the source term being

$$s_{\omega_0}(\mathbf{r}) = \frac{i\beta\omega_0}{C_P}e^{z/(2h)}\left(\omega_0^2\tilde{H}_s + g\frac{\partial \tilde{H}_s}{\partial z}\right). \quad (23)$$

Convolution of Eq. 11 with Eq. 23 with the result multiplied by $\exp\left[-z/(2h)\right]$ and its temporal part yields

$$p = \frac{\beta e^{-z/(2h)}}{4\pi C_P}\,\mathrm{Re}\left[-\frac{ie^{-i\omega_0 t}}{\sqrt{\omega_0^2-\omega_1^2}}\left(\hat{p}_a+\hat{p}_b\right)\right], \quad (24)$$

where

$$\hat{p}_a = \omega_0^2\int\frac{e^{i\omega_0\sqrt{\beta}R/c+z_0/(2h)}}{R}\tilde{H}_s d\mathbf{r}_0,$$

$$\hat{p}_b = g\int\frac{e^{i\omega_0\sqrt{\beta}R/c+z_0/(2h)}}{R}\frac{\partial\tilde{H}_s}{\partial z}d\mathbf{r}_0.$$

The above two integrals can be evaluated analytically as

$$\hat{p}_a(\mathbf{r}, z_s) = \omega_0^2 P_0 e^{z_s/(2h)} \frac{e^{i\omega_0\sqrt{\beta}R(x,y,z;0,0,z_s)/c}}{R(x,y,z;0,0,z_s)},$$
$$\hat{p}_b(\mathbf{r}, z_s) = -\frac{g}{\omega_0^2}\frac{\partial \hat{p}_a(r, z_s)}{\partial z_s}.$$

Equation 24 along with the radiation pattern for a monochromatic monopole radiator is plotted in Fig. 4. When the intensity of the source oscillates at a frequency lower than ω_1, as can be seen in Fig. 4(a), there exists a region separated by the curved line on the left of which the wave is evanescent. Outside the region the wave is progressive and its amplitude decreases along the y direction due to the spherical divergence and decreases exponentially along the z direction due to the density stratification. The curved line is part of the intersection line between the observation plane ($x_{obs} = 20$ km) and the evanescent cone surface, and it can be described by $z = \sqrt{-\hat{\alpha}(y^2 + x_{obs}^2)}$.

IV. HIGH FREQUENCY APPROXIMATION

The high frequency approximation can be carried out to separate the acoustic wave component from the gravity wave. The acoustic wave equation can then be written as

$$\left(\nabla^2 - \frac{1}{c^2}\frac{\partial^2}{\partial t^2}\right)\Pi = -\frac{\beta e^{z/(2h)}}{C_P}\frac{\partial H(\mathbf{r}, t)}{\partial t}, \qquad (25)$$

where $\Pi = \exp\left[z/(2h)\right] p_1$. Note that since the wave equation operator commutes with $\partial/\partial t$, it is advantageous to evaluate first the source term without the time differentiation obtaining the variable φ, and then Π can be found by $\Pi = -\partial\varphi/\partial t$.

A. cw laser beam directed along the z axis

Suppose a laser beam whose intensity is modulated at an angular frequency ω_0, located at $x = y = 0$ is directed along the z axis. The heating function for this source can be taken as

$$H(\mathbf{r}, t) = \frac{P_0}{2h} e^{-i\omega_0 t}\delta(x)\delta(y)e^{-z/h}. \qquad (26)$$

The heating function is taken to decay exponentially along the z axis following the distribution of the hydrostatic density ρ_0.

By using the Green's function for the three dimensional wave equation in free space $G_{\mathrm{WE}}(\mathbf{r}, t; \mathbf{r}_0, t_0)$, φ is found as

$$\varphi = \frac{\beta}{C_P}\int_0^t dt_0 \int_{-\infty}^{\infty} e^{z_0/(2h)} G_{\mathrm{WE}}(\mathbf{r}, t; \mathbf{r}_0, t_0) H(\mathbf{r}_0, t_0) d\mathbf{r}_0$$
$$= -\frac{\beta P_0}{8\pi C_P h} e^{-z/(2h)}\Lambda_{\omega_0}(t), \qquad (27)$$

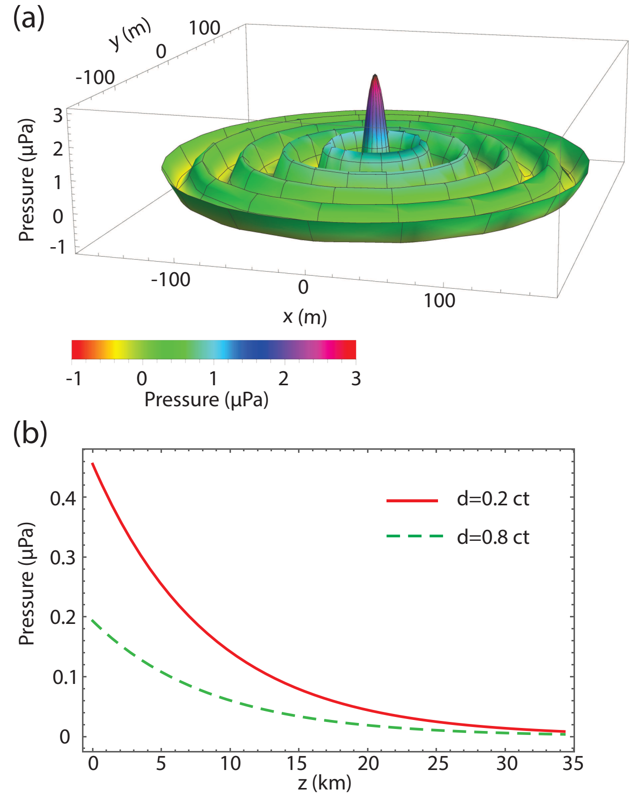

FIG. 5. (Color online) Distribution of the photoacoustic pressure (a) on the xy plane at $z = 0$ and (b) along the z axis for a modulated cw laser beam pointing upwardly. The laser intensity is modulated at $f_0 = 10$ Hz with $P_0 = 1$ kW and $t = 1$ s. Other parameters are the same as Fig. 3.

where

$$\Lambda_{\omega_0}(t) = e^{-i\omega_0 t}\int_{-\sqrt{(ct)^2-d^2}}^{\sqrt{(ct)^2-d^2}} \frac{e^{i\omega_0\sqrt{d^2+q_0^2}/c}}{\sqrt{d^2+q_0^2}} e^{-q_0/(2h)} dq_0, \qquad (28)$$

and $d = \sqrt{x^2 + y^2}$. The pressure can then be calculated via $p = -\exp\left[-z/(2h)\right]\partial\varphi/\partial t$, which gives

$$p = \frac{\beta P_0 e^{-z/h}}{8\pi C_P h}\mathrm{Re}\Bigg\{ -i\omega_0\Lambda_{\omega_0}(t) + \frac{c\left(e^{-\sqrt{(ct)^2-d^2}/(2h)} - e^{\sqrt{(ct)^2-d^2}/(2h)}\right)}{\sqrt{(ct)^2 - d^2}}\Bigg\}. \qquad (29)$$

As shown in Fig. 5(a), the wave described by Equation 29 resembles a two-dimensional cylindrical wave. It is well known that two-dimensional waves exhibit anomalous dispersion, that is, the wave changes its shape and forms a tail even if the wave speed is frequency-independent [28]. The geometric explanation for this behavior is that the wave received at a certain observation point can be regarded as the summation of three-dimensional spherical waves coming from successively more distant point sources along the vertical source

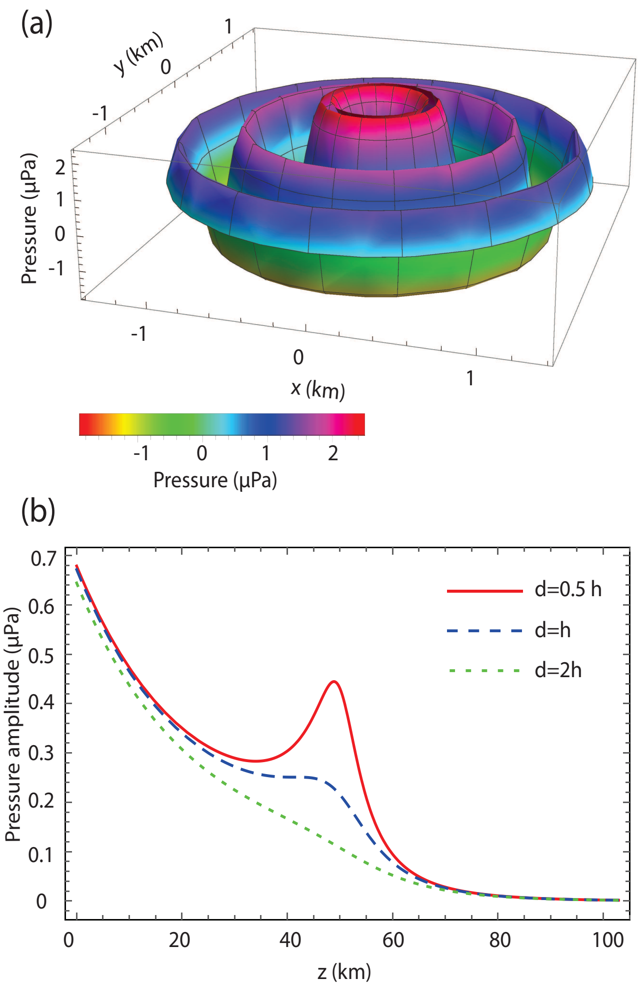

FIG. 6. (Color online) (a) Distribution of the photoacoustic pressure on the xy plane and (b) pressure magnitude along the z axis at $t = 10$ s for a point source oscillating at $f_0 = 1$ Hz. The point source is placed at $(0, 0, 50$ km$)$ with $P_0 = 1$ kW, and the observation plane is $0.2ct$ lower than the source. Other parameters are the same as given in Fig. 3. Plot (b) shows that there exist both a local maximum and minimum for pressure in the case of $d = 0.5h$, which evolve into a single saddle point for $d = h$.

line. Equation 28 describes such a consecutive summation with the difference being that the spherical wave is weighted by a factor $\exp[-q_0/(2h)]$ arising from density stratification. After the time differentiation, this extra factor results in a non-oscillatory term appearing in Eq. 29. It is noted that when the boundary condition is added, the magnitude of the weighting factor will be limited by $\exp[z_s/(2h)]$ and an controlled exponential growth is expected.

B. High frequency monochromatic monopole radiator

Consider the same heating function as Eq. 22 but with $\omega_0 \gg \omega_2$; its convolution with the Green's function G_{WE} yields

$$\begin{aligned} \varphi &= \frac{\beta}{C_P}\int_0^t\int_{-\infty}^{\infty} e^{z_0/(2h)} G_{\mathrm{WE}}(\mathbf{r}, t; \mathbf{r}_0, t_0) H(\mathbf{r}_0, t_0) d\mathbf{r}_0 dt_0 \\ &= -\frac{\beta P_0 e^{z_s/(2h)}}{4\pi C_P}\frac{e^{-i\omega_0(t-|\mathbf{r}-\mathbf{r}_s|/c)}}{|\mathbf{r}-\mathbf{r}_s|}. \end{aligned} \tag{30}$$

The pressure is thus obtained as

$$p = -\frac{i\omega_0 \beta P_0 e^{(z_s - z)/(2h)}}{4\pi C_P}\frac{e^{-i\omega_0(t-|\mathbf{r}-\mathbf{r}_s|/c)}}{|\mathbf{r}-\mathbf{r}_s|}. \tag{31}$$

Equation 31 shows that the amplitude of the photoacoustic pressure will increase exponentially as it approaches the ground as a result of density stratification of the medium. On the other hand, the wave experiences spherical divergence as it moves away from the source. The competition between the stratification increase and spherical divergence results in the appearance of local pressure maximum and minimum when the observation line is close to the vertical line where the source lies, which can be seen in Fig. 6(b). Specifically, the locations of the local maximum and minimum can be determined as

$$\begin{aligned} z_{\max} &= -h + z_s + \sqrt{h^2 - d^2}, \\ z_{\min} &= -h + z_s - \sqrt{h^2 - d^2}. \end{aligned}$$

V. SUMMARY

This paper gives a general differential equation that associates the generation and propagation of the atmospheric pressure perturbation with an optical driving force. Compared with the ordinary photoacoustic wave equation, the optically launched pressure perturbation in a stratified medium is related not only to the time derivative of the heating function but also its distribution along the stratified direction. The Green's functions for the governing equation in the frequency and time domains have been derived. Also, the reflection of the pressure wave by the earth ground has been shown to result in a "ringing-type" wave in addition to the "echo" wave corresponding to the Neumann boundary condition. Atmospheric response to pulsed and cw modulated radiation has been investigated. In all cases reported, there is invariably an exponential decrease in pressure upwardly along the vertical direction in addition to the geometric divergence. In contrast, the vertical velocity perturbation u_{1z} will grow exponentially as z increases to balance the decrease in the density ρ_0 and ensure that the vertical flux of horizontal momentum remains constant [29]. It is expected that the calculations presented here will aid in the understanding of the photoacoustic process in anisotropic medium, and bridge the fruitful photoacoustic applications with various atmospheric wave phenomena.

ACKNOWLEDGMENTS

The authors are grateful to the U.S. Department of Energy under Grant No. DE-SC0001082 for support of this research.

[1] A. G. Bell, Journal of the Society of Telegraph Engineers **9**, 404 (1880) .

[2] A. Rosencwaig, Optics Communications **7**, 305 (1973) .

[3] L. Xiong, W. Bai, F. Chen, X. Zhao, F. Yu, and G. J. Diebold, Proceedings of the National Academy of Sciences of the United States of America **114**, 7246 (2017) .

[4] A. C. Tam, Reviews of Modern Physics **58**, 381 (1986) .

[5] A. A. Oraevsky, S. L. Jacques, and F. K. Tittel, Applied Optics **36**, 402 (1997) .

[6] L. V. Wang and S. Hu, Science **335**, 1458 (2012) .

[7] R. Spalding, J. Tencer, W. Sweatt, B. Conley, R. Hogan, M. Boslough, G. Gonzales, and P. Spurny, Scientific Reports **7**, 41251 (2017) .

[8] M. C. Kelley and C. Price, Geophysical Research Letters **44**, 2987 (2017) .

[9] W. Bai and G. J. Diebold, Journal of Applied Physics **119**, 124904 (2016) .

[10] W. Bai and G. J. Diebold, Journal of the Acoustical Society of America **142**, 3796 (2017) .

[11] G. Chimonas and C. Hines, Journal of Geophysical Research **75**, 875 (1970) .

[12] T. Beer, Nature **242**, 34 (1973) .

[13] S. De Angelis, S. R. McNutt, and P. Webley, Geophysical Research Letters **38** (2011) .

[14] R. V. Row, Journal of Geophysical Research **72**, 1599 (1967) .

[15] G. J. Diebold, T. Sun, and M. I. Khan, Physical Review Letters **67**, 3384 (1991) .

[16] H. Erkol, E. Aytac-Kipergil, and M. B. Unlu, Physical Review E **90**, 023001 (2014) .

[17] A. R. Fisher, A. J. Schissler, and J. C. Schotland, Physical Review E **76**, 036604 (2007) .

[18] I. Tolstoy, Reviews of Modern Physics **35**, 207 (1963) .

[19] J. Lighthill, *Waves in Fluids* (Cambridge University Press, 1978) see pages 284-290 for the internal gravity wave and pages 237-245 for the phase and group velocities .

[20] V. Weston, Canadian Journal of Physics **39**, 993 (1961) .

[21] S. Egerev, Acoustical Physics **49**, 51 (2003) .

[22] T. Beer, *Atmospheric Waves* (John Wiley & Sons, 1974) see page 7 .

[23] F. Schmitz and B. Fleck, Astronomy and Astrophysics **337**, 487 (1998) .

[24] P. M. Morse and H. Feshbach, *Methods of Theoretical Physics* (McGraw-Hill Book Company, INC., 1953) see Eq. 7.2.18 in page 811 for the Green's function for the two-dimensional steady wave; pages 854-857 for the discussion of the solution to the Klein-Gordon equation.

[25] H. Bateman, *Tables of integral transforms*, Vol. 1 (McGraw-Hill Book Company) see Eq.59 in page 59 .

[26] A. D. Pierce, The Journal of the Acoustical Society of America **35**, 1798 (1963) .

[27] J. Bondurant and S. Fulling, Journal of Physics A: Mathematical and General **38**, 1505 (2005) .

[28] C. M. Bender, F. J. Rodriguez-Fortuno, S. Sarkar, and A. V. Zayats, Physical Review Letters **119**, 114301 (2017) .

[29] C. J. Nappo, *An Introduction to Atmospheric Gravity Waves* (Academic Press, 2013) see pages 26-30 .